Sensors and Actuators B 250 (2017) 692–702

Contents lists available at ScienceDirect

Sensors and Actuators B: Chemical

journal homepage: www.elsevier.com/locate/snb

Flower-like ZnO hollow microspheres loaded with CdO nanoparticles as high performance sensing material for gas sensors

Tianshuang Wang[a], Xueying Kou[a], Liupeng Zhao[a], Peng Sun[a,*], Chang Liu[a,b,c], Yue Wang[b], Kengo Shimanoe[c], Noboru Yamazoe[c], Geyu Lu[a,*]

[a] State Key Laboratory on Integrated Optoelectronics, College of Electronic Science and Engineering, Jilin University, 2699 Qianjin Street, Changchun 130012, People's Republic of China
[b] State Key Laboratory Supramolecular Structure and Materials, College of Chemistry, Jilin University, 2699 Qianjin Street, Changchun 130012, People's Republic of China
[c] College of Energy and Material Science, Faculty of Engineering Science, Kyushu University, Kasyga-shi, Fukuoka 816-8580, Japan

ARTICLE INFO

Article history:
Received 21 November 2016
Received in revised form 23 March 2017
Accepted 16 April 2017
Available online 19 April 2017

Keywords:
CdO/ZnO composites
Hollow microspheres
n-n Heterojunction
Gas sensors
Low detection limit

ABSTRACT

CdO decorated flower-like ZnO hollow microspheres were successfully prepared via a two-step hydrothermal strategy. CdO nanoparticles (~12 nm) equably loaded on the surfaces of ZnO nanosheets, which could be clearly observed from SEM and TEM images. The results of X-ray photoelectron spectroscopy and H_2 temperature-programmed reduction (H_2-TPR) indicated that the amount of chemisorbed oxygen was increased after the introduction of CdO nanoparticles. Compared with the flower-like ZnO hollow microspheres, the 2.6 mol% CdO:ZnO heterostructure composites exhibited highest response (65.5) to 100 ppm ethanol at 250 °C, which was about 16 folder higher than that of pure ZnO at the same operating temperature of 250 °C. Significantly, the detection limit of the 2.6 mol% CdO:ZnO heterostructure could reach ppb level (500 ppb). The mechanism of the enhanced ethanol sensing was also discussed systematically.

1. Introduction

Up to now, the research of gas sensors has attracted continually increasing interest because of their extensive applications [1–3]. Among the various types of gas sensors, the semiconductor oxides sensors hold a central position due to their low cost, high sensitivity, simplify in fabrication and compatibility with modern electronic devises [4,5]. It is known to all that the fundamental operating mechanism is the remarkable resistance change caused by the surface reaction upon exposure to different gas ambients. Consequently, for the purpose of improving the gas sensing properties, various effective approaches have been centered on the design of the semiconductor oxides with excellent sensing performance and numerous results have demonstrated that the sensing performance of metal semiconductors oxide is not only highly dependent on their microstructures [6,7], but also related to their further functionalization with metal elements [8–11], heterogeneous oxide [12,13], and so on. To date, among these strategies, expanding the sensing materials from single component metal semiconductor oxide to multicomponent heterostruture has become more and more fascinating, such as ZnO/SnO_2 [14], α-Fe_2O_3/ZnO [15], NiO/ZnO [16], α-Fe_2O_3/SnO_2 [17], CdO/In_2O_3 [18], and CuO/ZnO [19] have been successfully prepared and have indeed improved the sensing properties, because they are supposed to integrate the physical and chemical properties of their individual component. The constant need for gas sensors with high sensitivity, low operating temperature, and good stability continues to stimulate the progress of gas sensing. Therefore, it is very important to make efforts in the rational design and synthesis of new-type composites.

As an important n-type semiconductor with wide band-gap of ~3.4 eV, ZnO has been regarded as the most potential sensing material because it has response to the target gases and easily for synthesizing [20]. It is found that hierarchical structure, as a higher dimension of micro- and nanostructures assembled from low dimensional blocks, has been used to improve sensitivity of ZnO [21,22]. However, the pure ZnO as sensing material still has the following problems: low response, worse selectivity and high operating temperature. Consequently, in order to further improve the gas sensing properties of pure ZnO nanostructure, heterostructure formation between ZnO and other oxide semiconductors has been developed [16,19]. Cadmium oxide (CdO), as a n-type semi-

* Corresponding authors.
E-mail addresses: spmaster2008@163.com (P. Sun), lugy@jlu.edu.cn, 181306776@qq.com (G. Lu).

http://dx.doi.org/10.1016/j.snb.2017.04.099
0925-4005/

conductor oxide with a narrow band gap of ~2.4 eV [23] has the following advantages: high carrier mobility and high conductivity (103 Ω^{-1} cm^{-1}), due to its native defects of oxygen vacancies in the lattice [23–26]. Recently, some studies have demonstrated that combining ZnO with CdO could improve gas sensing properties compared with single component of oxide. For example, Kim et al. [27] have synthesized ZnO/CdO core/shell nanorod arrays via three kinds of method, which demonstrated a high sensitivity towards ethanol at high operating temperature. Ban et al. [28] have manifested CdO nanoflake arrays on ZnO nanorods arrays was a promising gas sensing material for detection of diethyl ether. Although some studies have reported on CdO/ZnO composites gas sensors, there is no report on 3D ZnO hierarchical structure decorated by 0D CdO nanoparticles. The distinct feature of this kind of heterostructur is highly advantageous for gas sensors due to the synergistic integration of the merits of individual components and the formation of heterostructure. In addition, this kind of heterostructur can maintain a well-dispersed configuration after decorating nanoparticles, which is a favorable structure for facile gas permeation and results in both of them are highly accessible for gas detection [29,30].

Inspired by these, we present a strategy for the preparation of CdO-decorated flower-like ZnO hollow microspheres composites. First, the flower-like ZnO hollow microspheres were prepared via a hydrothermal route. After that, CdO nanoparticles with a diameter of ~12 nm were decorated on the surfaces of ZnO nanosheets by hydrothermal process. Furthermore, nanoparticles are well-distributed on the ZnO hollow spheres. A systematically comparative gas sensing investigation between the pure ZnO and CdO/ZnO hollow microspheres composites was performed. These results indicated that the CdO/ZnO hollow microspheres composites with a Cd:Zn molar ratio of 2.6:100 showed the highest response to ethanol, which was nearly ~16 fold higher than that of pure ZnO at 250 °C. The dramatic improvement in gas sensing properties may be attributed to the change of the n-n heterojunction barrier height at the different gas atmospheres and the synergetic effect between CdO and ZnO.

2. Experimental

2.1. Materials synthesis

2.1.1. Preparation of the flower-like ZnO hollow microspheres

All the reagents were analytical grade and were used as received without further purification. The flower-like ZnO hollow microspheres were synthesized by facile one-step hydrothermal route. First, 0.439 g of $Zn(CH_3COO)_2{\cdot}2H_2O$, 0.4 g of glycine and 0.4 g of $Na_2SO_4{\cdot}10H_2O$ were completely dissolved into a mixture of 15 mL of deionized water and 10 mL of ethanol at the same time, under vigorous stirring for 5 min. Then 0.4 g of NaOH was added into the prepared solution with magnetic stirring for about 1 h. Afterward the mixed solution was transferred into a 45 mL Teflon-lined stainless steel autoclave and heated at 180 °C for 12 h. After the autoclave cooled naturally down to room temperature, the precipitates were collected by centrifugation, washed several times with distilled water and absolute ethanol respectively, and dried in air at 80 °C for 12 h, and calcined at 400 °C for 2 h.

2.1.2. Synthesis of the CdO/ZnO heterostructure composites

A series of 0, 0.4, 0.9, 2.6, 4.4 mol% CdO:ZnO heterostructure composites (the molar percentage was defined as the ratio of the moles of CdO to that of ZnO) were also synthesized via a simple hydrothermal method, which can be described briefly as follows: First, 30 mg of the obtained ZnO powders mentioned above were dispersed in 30 mL of DMF under continuous magnetic stirring to form a homogeneous solution. Then a certain amounts of $Cd(NO_3)_2{\cdot}4H_2O$ and CH_4N_2S were added into the prepared homogeneous solution with stirring for 10 min. Afterwards, 300 μL of isopropanol was added into the solution, which was stirred for 10 min and ultrasonicated for 30 min. After that the solution was transferred into a 45 mL Teflon-lined stainless steel autoclave and heated at 160 °C for 10 h, followed by cooling to room temperature naturally. The pre-synthesized precipitates were centrifuged and rinsed several times with deionized water and ethanol alternately, and dried in air at 60 °C for 10 h. Finally, the as-prepared precursors were annealed under an air atmosphere at a temperature of 500 °C for 3 h in an electronic oven with a temperature ramp of 1 °C min^{-1} to convert CdS to CdO.

2.2. Materials characterization

Crystallinity and composition of the final samples were identified by X-ray powder diffraction (XRD) (Rigaku D/Max–2550 V X-ray diffractometer) using high-intensity Cu Kα radiation (λ = 1.5403 Å) in the range of 20°–70° (2θ) with a scanning speed of 2° min^{-1}. The morphology and microstructure of the products were directly observed by field-emission scanning electron microscopy (FESEM JEOL JSM-7500F, operated at an accelerating voltage of 15 kV). Transmission electron microscopy (TEM) and high-resolution transmission electron microscopy (HRTEM) were recorded on a JEOL JSM-2100F operating at an accelerating voltage of 200 kV. X-ray spectrometry (EDS) pattern were also observed through the attachment of TEM. The X-ray photoelectron spectroscopy (XPS) measurements were performed with Al Kα X ray source. The XPS Peak 4.1 software was used to fit peaks in the XPS spectra. The H_2 temperature-programmed reduction (H_2-TPR) was investigated by employing 100 mg sample in each measurement. The samples were firstly pretreated by Ar at 300 °C for 30 min, then cooled down to room temperature, and followed by turning the flow of 10% H_2/Ar into the system with a flow rate of 30 mL/min. The samples were heated from room temperature to 750 °C at a rate of 10 °C/min.

2.3. Fabrication and measurement of the gas sensor

The schematic of the fabricated gas sensor was shown in Fig. S1 and the fabrication process of the sensor device could be described as follows: First, an appropriate amount of the pure ZnO and CdO/ZnO hollow microspheres composites samples were thoroughly mixed with deionized water in a motor to form the homogeneous paste. Then, the paste was coated onto an alumina tube (external diameter: 1.2 mm, internal diameter: 0.8 mm, and length: 4 mm; a couple of Au electrodes were previously printed on the end of the tube, and each electrode was connected with a pair of Pt wires) to form a thick sensing film. After that, the device was calcined at 400 °C for 2 h. A Ni—Cr alloy coil was inserted through the alumina tube as a heater, and we could control the operating temperature by tuning the heating current flowed through the heater. Finally, the gas sensor was obtained by aging at 100 mA relative current for 5 days.

The sensing performances of sensors were measured by a static testing system [31]. The humidity was maintained at 30% RH. The response (S) of the sensor was defined as the ratio of Ra/Rg, where Ra and Rg were the sensor resistance in the air and target gases. The response time (τ_{res}) and recovery time (τ_{rec}) were defined as the time taken by the sensor to achieve 90% of the total resistance change in the case of adsorption and desorption, respectively.

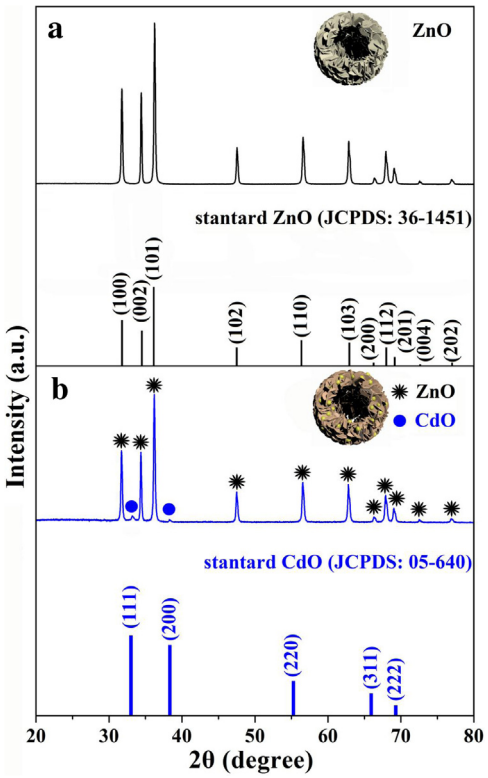

Fig. 1. (a) XRD patterns of the as-prepared flower-like hollow ZnO microspheres; (b) The 2.6 mol% CdO:ZnO composites.

3. Results and discussion

3.1. Structural and morphological characteristics

The XRD pattern (Fig. 1) showed the crystal structure and phase purity of as-synthesized flower-like ZnO hollow microspheres and the 2.6 mol% CdO:ZnO heterostructure composites. As can be seen in the obtained XRD patterns in Fig. 1a, the first step hydrothermally synthesized and calcined products were highly consistent with the wurtzite hexagonal structure (a = 3.25 Å, c = 5.21 Å) of ZnO (JCPDS Card No. 36-1451). As for the 2.6 mol% CdO:ZnO heterostructure composites, the crystal phases in Fig. 1b were the mixed oxides of CdO and ZnO. Apart from the peaks that belong to the pure ZnO, only two diffraction peaks left in this pattern could be matched with the (111) and (200) planes indexed to the cubic structure (a = 4.695 Å) of CdO (JCPDS Card No. 05−640). By contrast, the peaks of CdO were weaker than those of ZnO in the composite, probably because of the component of CdO:ZnO composites was mostly ZnO and the amounts of CdO in CdO/ZnO composites were close to the limit of detection of XRD analysis. Above all, no diffraction peaks belonging to any other impurities could be detected, which indicated that the final product was a mixture of CdO and ZnO with separate phases.

The low magnification FESEM image (Fig. 2a) of the as-obtained ZnO samples clearly provided that the products consists of numerous flower-like ZnO microspheres with uniform size (~3 μm) without other morphologies. The high magnification FESEM images in Fig. 2(b) and (c) confirmed that the ZnO microspheres were actually hierarchical hollow microstructures, which were composed of 2D nanosheets with a thickness of ~60 nm. In addition, the nanosheets of ZnO hollow microspheres had a relatively smooth surface. According to Figs. 2d and S3, the size and distribution of the microstructures were maintained after the introduction of CdO. Besides that, the high magnification FESEM image Fig. 2(e) exhibited detailed morphological information on a single ZnO hollow microsphere with CdO nanoparticles decorated on its surface. The surfaces of the 2.6 mol% CdO:ZnO heterostructure composites became much coarser compared with the pure ZnO hollow microspheres (Fig. 2(f)), which might be ascribed to the surfaces of the ZnO nanosheets were successfully decorated with the secondary CdO nanoparticles. Furthermore, from the higher magnification FESEM image (Fig. 3a) of the surfaces of the 2.6 mol% CdO:ZnO heterostructure composites, we could further confirm that massive CdO nanoparticles were coated on the surfaces of ZnO nanosheets with a size of ~12 nm. These rough surfaces were more benefit for gas detection, owing to heterostructures could provide more active sites and high specific surface area required for excellent gas sensing properties [32].

The TEM and HRTEM observations were also performed to further investigate the interior and the crystalline structure of the 2.6 mol% CdO:ZnO heterostructure composites. From the enlarged TEM observation of Fig. 3b, the ZnO nanosheets and the CdO nanoparticles could be clearly identified, and the surfaces of the ZnO nanosheets were not completely enclosed by CdO nanoparticles. In addition, the TEM image in Fig. 3h indicated that the CdO/ZnO heterostructure composites were still hollow microstructures, where the size and exterior structure of the CdO/ZnO heterostructure composites were similar to the observation of FESEM. The fringe spacing of 0.277 nm clearly observed in the HRTEM image (Fig. 3d) agreed well with the spacing of the (100) lattice plane of the wurtzite hexagonal structure of ZnO (JCPDS Card No. 36-1451). And the apparent lattice fringes observed from the HRTEM images (Fig. 3(e–g)) presented that the lattice spacing of adjacent lattice planes were about 0.234 and 0.232 nm, which corresponded to the distance between the (200) plane of the cubic structure of CdO (JCPDS Card No. 05-640). Fig. 3(i–k) displayed the corresponding elemental spacial distribution of the individual CdO/ZnO heterostructure composites shown in Fig. 3h.

3.2. Composition analysis

The surface elemental composition and chemical status of the as-prepared CdO/ZnO heterostructure composites were further investigated by XPS, and the corresponding results were presented in Fig. 4. All of the binding energies in the XPS analysis were corrected by the C 1s peak (set at 284.6 eV). In the wide survey scan of XPS spectra (Fig. 4a), Zn, Cd, C and O could be found in the final product. As depicted in Fig. 4b, the two strong peaks centered at 412.2 and 405.4 eV correspond to the Cd 3d3/2 and Cd 3d5/2, respectively, indicating the existence of Cd^{2+} in the calcined product [33]. As for surface resistance-type metal oxide semiconductors, the gas sensing properties were closely related to the ability of absorb and ionize oxygen species. Therefore, the O 1s spectrum of the as-prepared single-component hollow ZnO microspheres and 2.6 mol% CdO:ZnO heterostructure composites were exhibited in Fig. 4(c and d), respectively. The O 1s peak was fitted to three peaks (O_C, O_V, and O_L) by Gaussian simulation peaks, which could be attributed to three kinds of oxygen species: the O_C component was assigned to chemisorbed oxygen species, the middle of the three curves was O_V component in oxygen vacancy regions within the ZnO and CdO, and the O_L component was identified to the lattice oxygen [34]. Their binding energies and the relative percentage of each component were listed in Table 1. It could be found that the relative percentage of O_C component was about 52.7% in the heterostructure composites, which was greatly increased comparison with that (~13.4%) in the single-component ZnO hollow microspheres. This indicated that the surface of the composites had the ability of adsorbing chemisorbed oxygen species during the oxidation-reduction reaction. Consequently, the sensing prop-

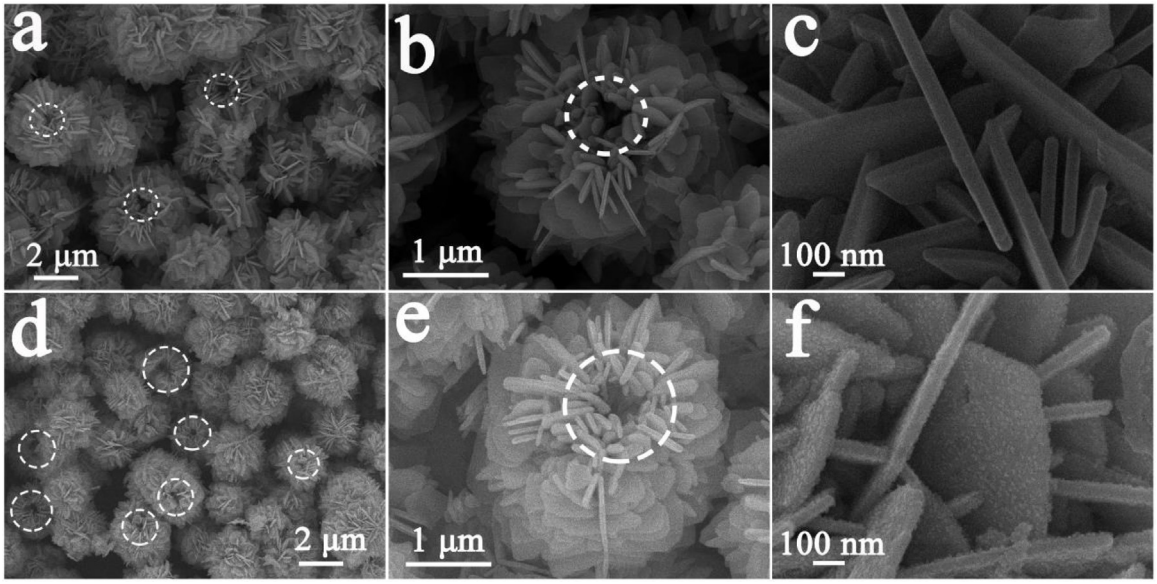

Fig. 2. Typical FESEM images of the as-prepared products (a–c) flower-like hollow ZnO microspheres; (d–f) the 2.6 mol% CdO:ZnO composites.

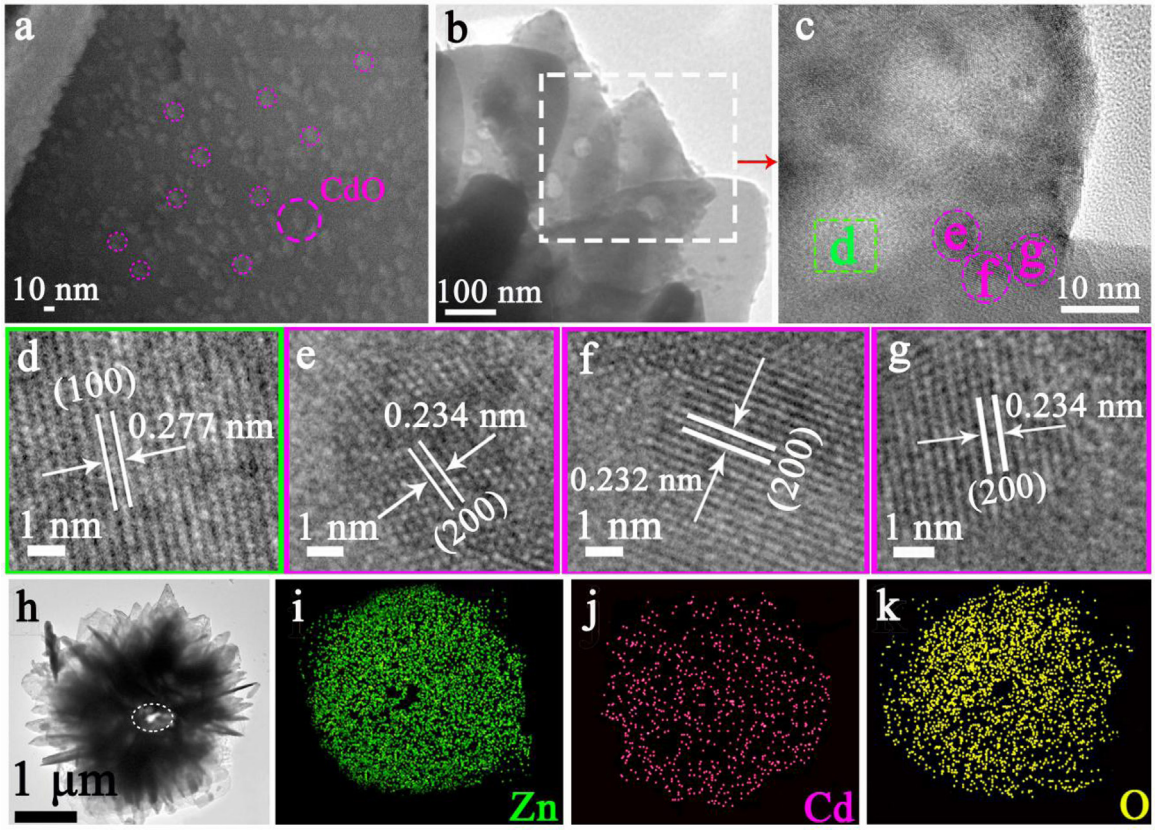

Fig. 3. (a,b) Typical FESEM and TEM images of the 2.6 mol% CdO:ZnO composites; (c) HRTEM image of the marked section in (b); (d–g) Magnified HRTEM images from marked fringe of (c); (h) TEM image of an individual 2.6 mol% CdO:ZnO composites; (i–k) Corresponding elemental mapping showing the dispersion of Zn, Cd and O elements.

Table 1
Fitting Results of O 1s XPS Spectra of the Two Samples.

Sample	Oxygen species	Binding energy (eV)	Relative percentage (%)
Flower-like ZnO hollow microstructure	O_C (Chemisorbed)	532.3	13.4
	O_V (Vacancy)	531.5	30.1
	O_L (Zn-O)	530.3	56.5
The 2.6 mol% CdO:ZnO heterostructure composites	O_C (Chemisorbed)	532	52.7
	O_V (Vacancy)	531	22.4
	O_L (Zn-O and Cd-O)	530.3	24.9

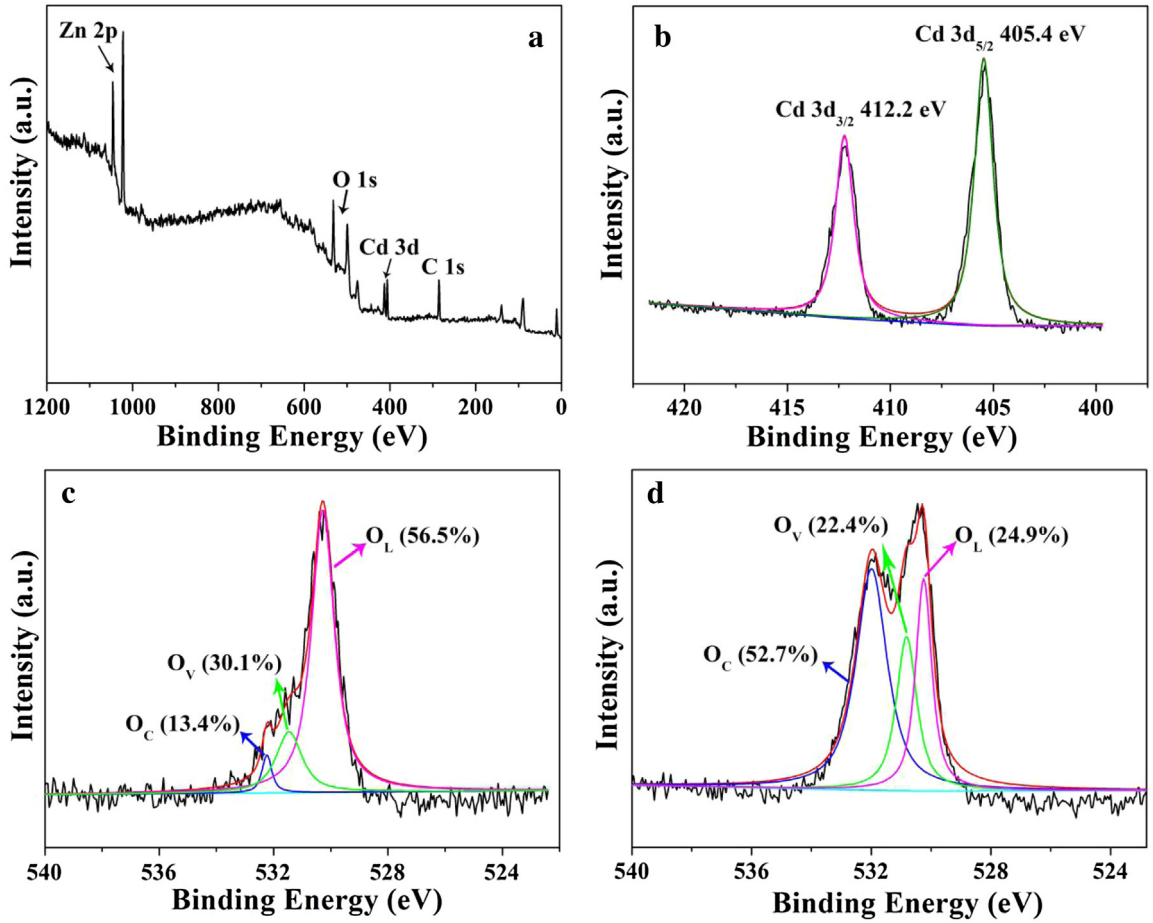

Fig. 4. XPS spectra of (a) the full range survey; (b) Cd 3d of CdO/ZnO composites; (c) O 1s spectra of single-component flower-like ZnO microspheres; (d) O 1s of the as-synthesized 2.6 mol% CdO:ZnO heterostructure composites.

erties may be enhanced due to the increasing in amount of absorbed oxygen.

4. Gas sensing application

4.1. Gas sensing properties

As is well-known, the response of a semiconductor gas sensor is highly influenced by the operating temperature. In order to explore the relationship between gas response and operating temperature as well as the optimal ratio of the moles of CdO to that of ZnO, a function of gas responses to operating temperatures of the sensors based on the pure ZnO and all CdO/ZnO heterostructure composites (with different moles ratio of CdO to ZnO) to 100 ppm ethanol were carried out in Fig. 5a. Obviously, the volcano-shaped correlation between gas response and operating temperature was observed for every sample, and this phenomenon could be explained as follows: At the beginning, with increasing the operating temperature, the ion sorption of oxygen active sites will quickly increase, leading to improved response. While beyond the optimal operating temperature, the response decreased with further increasing the operating temperature, which may result from two factors. The one is that the number of ethanol adsorption active sites decreasing. The other possibility is that the adsorption ability of target gas molecules was lower than that of desorption and led to the utilization rate of sensing material decreasing at such high temperatures [35–37]. The maximal gas response of pure ZnO hollow microspheres was 7.6 at 300 °C. In contrast with pure ZnO, the gas responses of sensors based on the 0.4 mol%, 0.9 mol%, 2.6 mol%, and 4.4 mol% CdO:ZnO heterostructure composites to 100 ppm ethanol at 250 °C were 12.3, 35.2, 65.5, and 23, respectively. The result revealed that the sensor based on the 2.6 mol% CdO:ZnO heterostructure composites showed the highest gas response to 100 ppm ethanol and the value was about 16 times higher than that of pure ZnO at the same operating temperature of 250 °C. In addition, the optimal operating temperature of the CdO/ZnO heterostructure composites (250 °C) was lower than that of pure ZnO (300 °C), indicating the catalytic role of transition metal oxides (CdO) to promote gas sensing reaction at lower operating temperature. The introduction of CdO is known to reduce the optimal operating temperature of CdO/ZnO nanocomposites [27,38,39]. The phenomenon can be explained by the effect of transition metal oxides (CdO) catalyst for partial oxidation of volatile organic components (VOCs) [40]. Besides, the response of pure CdO nanoparticles is much lowest than the other sensors (Fig. S5(a)). We also found that the gas response of the 4.4 mol% CdO:ZnO heterostructure composites toward 100 ppm ethanol at 250 °C would decrease, we thought it was due to the CdO nanoparticles could not be uniformly coated and showed significant aggregation at interface (shown in Fig. S4).

In addition, selectivity is an important criterion for gas sensors in practical use. Therefore, the gas responses of sensors based on the pure ZnO and all CdO/ZnO heterostructure composites (with different moles ratio of CdO to ZnO) to 100 ppm of various target gases were investigated at 250 °C, the results of which were summarized in Fig. 5b. It can be clearly observed that all CdO/ZnO heterostructure composites (with different moles ratio of CdO to

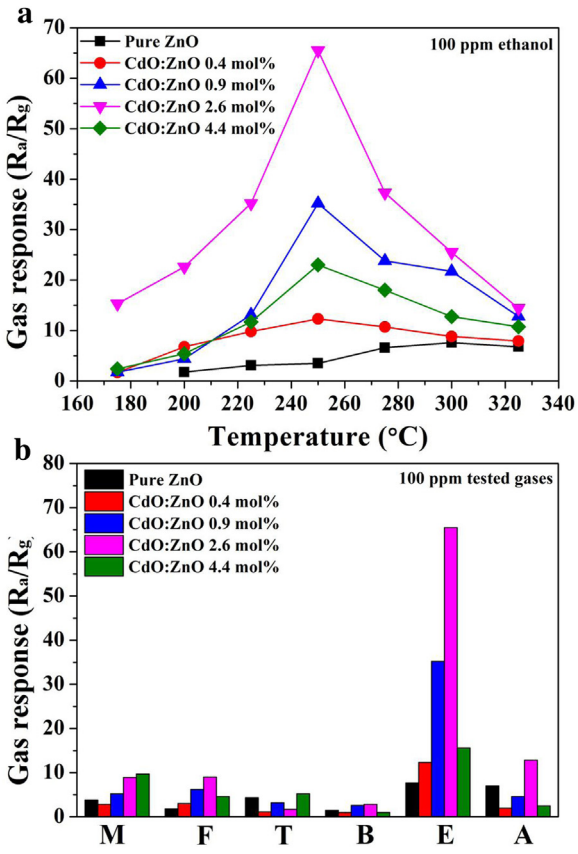

Fig. 5. (a) Gas responses of the sensors based on the pure, 0.4 mol%, 0.9 mol%, 2.6 mol%, and 4.4 mol% CdO:ZnO composites vs operating temperatures to 100 ppm ethanol. (b) Gas responses of five sensors to 100 ppm various target gases at 250 °C (M, methanol; F, formaldehyde; T, toluene; B, benzene; E, ethanol; A,acetone;).

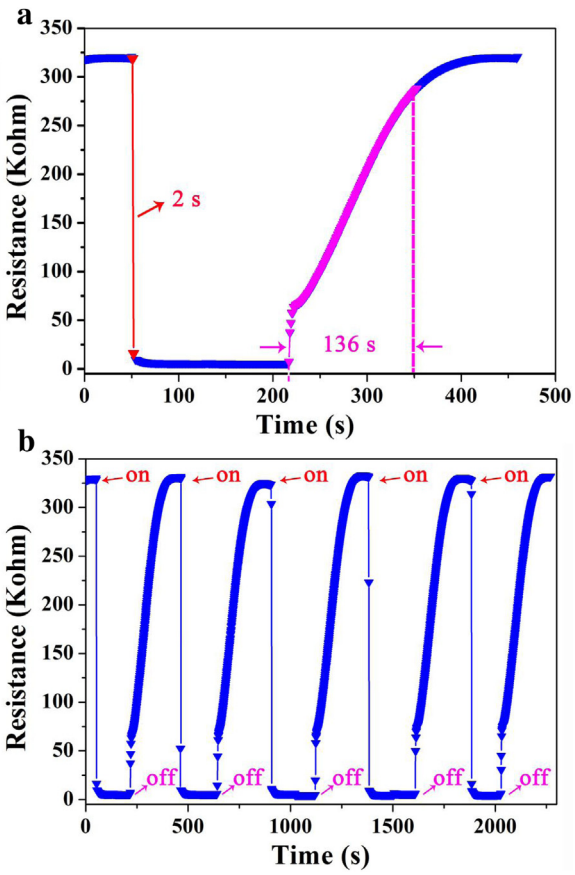

Fig. 6. (a) Response and recovery curves of the sensor based on the 2.6 mol% CdO:ZnO composites and (b) five reversible cycles to 100 ppm ethanol at 250 °C.

ZnO) exhibited the maximum response to ethanol gas, especially for the sensor based on the 2.6 mol% CdO:ZnO heterostructure composites, where its response to ethanol is 5.1–38.5 times higher compared to the other gases studied in our work, while the ratio was only about 1.1–5.3 for the pure ZnO sensor. And the selectivity to target gases of CdO nanoparticles is exhibited in Fig. S5(b). The result indicated that the synthesized CdO/ZnO heterostructure composites could obviously improve the selectivity of the hollow ZnO-based sensor to ethanol. It is well known that gas-sensing properties are dominantly controlled by the surface adsorption which makes the surface energy and the conductance change. Namely, the selectivity of the sensor is influenced by several factors such as the LUMO (lowest unoccupied molecule orbit) energy of gas molecule, the amount of gas adsorption on the surface of sensing material, and the operating temperature. At the same operating temperature, if the value of LUMO energy of tested gas is lower, the energy needing for the gas sensing reaction will be reduced and the sensing signal can be enhanced. So the sensor shows high sensitivity and good selectivity toward the gas with low LUMO energy. The good selectivity to ethanol observed here is likely to be the result of two factors. First, it has been demonstrated that the LUMO energy of ethanol (0.126 eV) is lower than the other common VOCs (such as methanol (0.197 eV), acetone (0.205 eV), formaldehyde (0.219 eV)) [41–44]. Based on above, the sensor based on CdO/ZnO composites exhibited good selectively to ethanol. Second, the introduction of CdO nanoparticles enhanced the catalytic activity of composites [45–47]. This means that the tested gases are activated and the reaction between the activated fragments of the gas and adsorbed oxygen species is facilitated. Due to the low LUMO energy, ethanol molecules are easier to activate which leads to high response and good selectivity. Certainly, in order to clarify the mechanism of selectivity to ethanol, further researches are being carried out.

The dynamic response and recovery curve of the 2.6 mol% CdO:ZnO heterostructure composites toward 100 ppm ethanol at 250 °C was displayed in Fig. 6a. It can be apparently observed that the resistance decreased immediately upon exposure to ethanol and the time taken was as low as 2s in this process. However, the recovery time was within 136s for ethanol. Fig. 6b exhibited the five reversible cycles of the response-recovery curve, it indicated that the 2.6 mol% CdO:ZnO heterostructure composites had a stable and repeatable characteristic as sensing material. Table 2 shows a comparison between the sensing properties of the sensor fabricated in this study and some ethanol gas sensors based on ZnO. The results confirmed that the gas sensor based on the 2.6 mol% CdO:ZnO heterostructure composites had a comparable or higher response, a faster response time at a relatively lower working temperature [16,22,27,48–54].

The response behaviors of gas sensors based on the pure ZnO and 2.6 mol% CdO:ZnO heterostructure composites to different concentration of ethanol at their optimal operating temperature (presented in Fig. 7a). Obviously, the responses of sensor devices exhibited a stepwise distribution by the increasing of ethanol concentration, this situation could be explained as follows: more and more ethanol molecules could participate in the surface reaction process and leading to the remarkable increase in gas response [55]. In addition, the gas sensing performances of sensors based on the pure and 2.6 mol% CdO:ZnO heterostructure composites to low ethanol concentrations were shown in the insert of Fig. 7a. It could be found that the sensor based on the 2.6 mol% CdO:ZnO heterostructure composites had ppb-level detection limit when compared with the pure ZnO. Fig. 7b depicted that the tem-

Table 2
Comparison of gas sensing performances of ethanol gas sensors based on ZnO.

Materials	Temperature (°C)	Concentration (ppm)	Response (R_a/R_g)	Response time (s)	Recovery time (s)	Reference
Hierachical hollow ZnO microspheres	275	100	8	1	19	[22]
Au-loaded ZnO hollow microspheres	325	200	14.5	1	30	[48]
Tb doped ZnO	280	100	~52	~4	~16	[49]
1% Cd-doped ZnO thin films	250	100	52%	30	53	[50]
SnO_2/ZnO heterostructure nanofibers	300	100	79	25	9	[51]
α-Fe_2O_3/ZnO hierachical nanostructures	370	100	53.6	6	7	[52]
NiO/ZnO nanostructures	200	100	16	6	22	[16]
Mn_3O_4/ZnO nanobelts	400	100	30	–	–	[53]
ZnO/CdO core/shell nanorod arrays	375	3	75	–	–	[27]
CdO/ZnO thin film	100	100	6	48	60	[54]
CdO/ZnO composites microspheres	250	100	65.5	2	136	This work

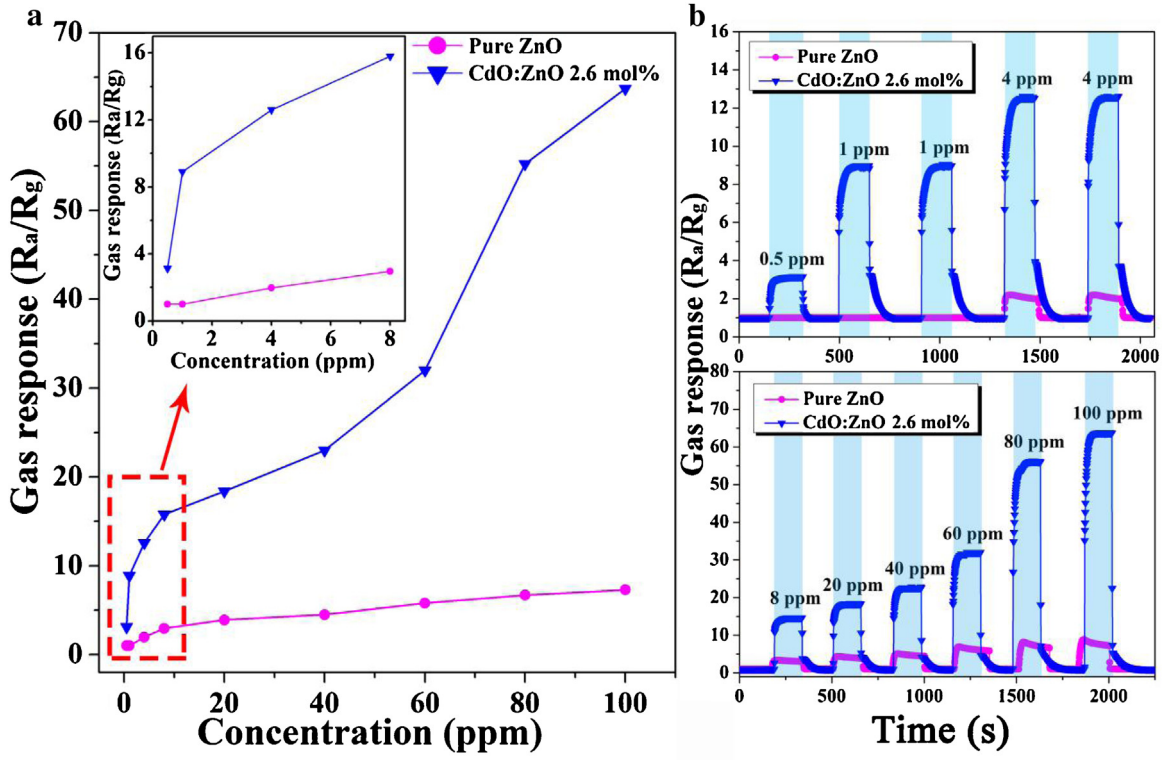

Fig. 7. (a) Responses vs ethanol concentration for the pure ZnO at 300 °C and the 2.6 mol% CdO:ZnO composites at 250 °C; (b) Real-time response curves of the sensors based on the pure ZnO and 2.6 mol% CdO:ZnO composites in the ethanol concentration range of 0.5–4 ppm and 8–100 ppm.

poral response and recovery curves by systematically exposing the two types of sensor devices to ethanol over a concentration range of 0.5–4 ppm and 8–100 ppm at the operating temperature. Apparently, the two types of sensor devices exhibited an excellent response and recovery upon exposure to different ethanol concentrations. Moreover, the 2.6 mol% CdO:ZnO heterostructure composites still had a response of 3.1 when the ethanol concentration was as low as 500 ppb, indicating the ultra-low detection limit of the heterostructure composites.

The long-term stability of sensor using 2.6 mol% CdO: ZnO heterostructure composites was investigated, as illustrated in Fig. 8, an experiment on the long-term stability of the sensor based on composites response to 100 ppm ethanol and the resistance in air atmosphere (Ra) was carried out at 250 °C over 30 days, which further indicated the extraordinary long-term stability of the sensing device. These favorable gas sensing properties might make the present nanomaterials to be particularly attractive as a promising practical sensor.

4.2. Gas-sensing mechanism

The gas-sensing mechanism of *n*-type semiconductor oxides is usually explained by the classical model of an electron depletion layer generated by the adsorption and desorption process of oxygen molecules on the surfaces of sensing materials [56]. When the gas sensor is exposed to fresh air, oxygen molecules will be adsorbed onto the surfaces of the sensing materials and capture free electrons from the conduction band of the sensing materials to form the oxygen adsorbents (O_2^-, O^- or O^{2-}), giving rise to a thick electron depletion layer on the surface, leading to a relatively high resistance. When the material is exposed to reducing gases, for instance, the ethanol molecules will react with the oxygen species on the surface and release electrons back into the conduction band of the semiconductor oxides, thereby decreasing the thickness of the depletion layer and increasing conductivity. The reaction is

$$CH_3CH_2OH + 7O^-(ads) \rightarrow 2CO_2 + 3H_2O + 7e^- \quad (1)$$

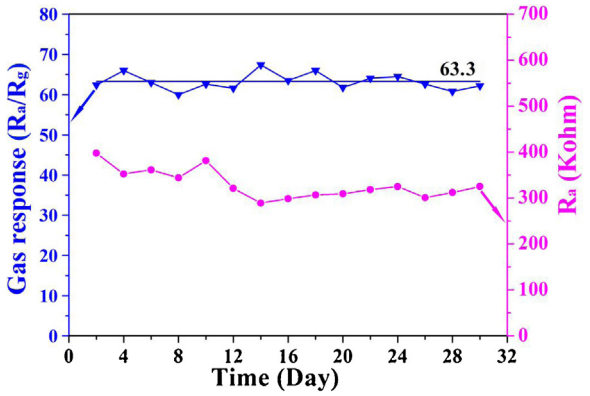

Fig. 8. Long-term stability of the gas sensor based on the 2.6 mol% CdO:ZnO composites measured at the operating temperature of 250 °C.

The sensor based on the CdO/ZnO heterostructure microspheres exhibits a remarkable improvement in gas-sensing properties are most likely to be ascribed to the following aspects: First of all, in our study, both CdO and ZnO are n-type semiconductor oxides, the energy band structure of the CdO/ZnO heterojunction can be schematically depicted in Fig. 9(a and b), in which Φ_{eff} is the effective barrier height. The work function of ZnO and CdO is 5.2 eV and 8.6 eV and the band gap of the two oxides is 3.4 eV and 2.4 eV, respectively [57,58]. So electrons will flow from ZnO to CdO, which will result in the formation of the hole depletion layer in ZnO nanoplates and electron accumulation layer on the surface of CdO. This will lead to the increase in amount of chemisorbed oxygen, which conforms to the XPS results and the theory analysis. Thus, as the sensors are exposed to ethanol, more absorbed oxygen species will take part in the reaction with organic molecules and more trapped electrons are released back into the conduction band simultaneously. Thereby, a decrease in the thickness of the electron

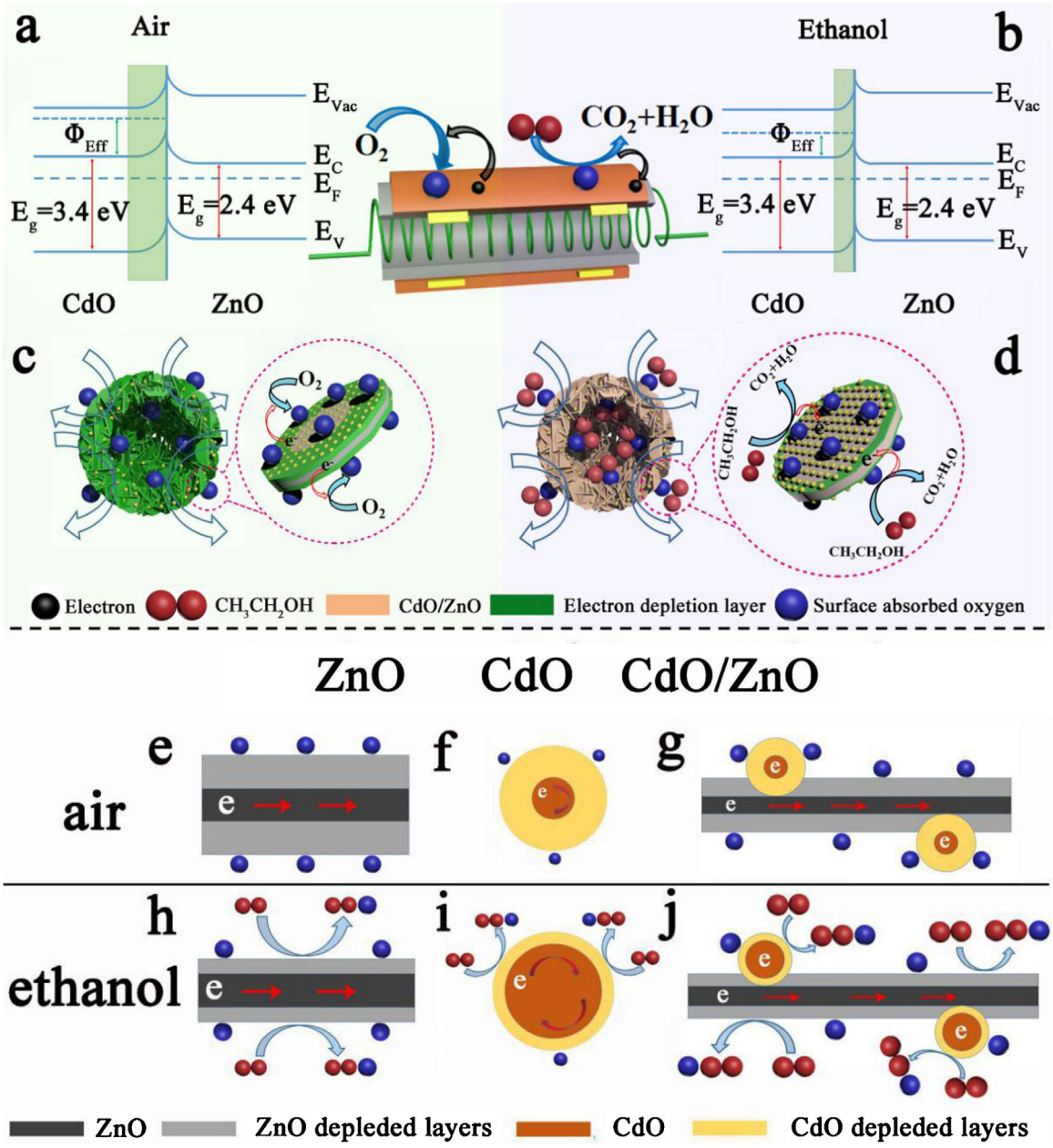

Fig. 9. (a and b) Schematic diagram illustrating the energy band structure of CdO/ZnO heterostructure in air and ethanol gases; (c and d) The plausible reason for exhibiting a high ethanol response; Schematic diagrams of ZnO, CdO and CdO/ZnO (e–g) in air; (h–j) in ethanol.

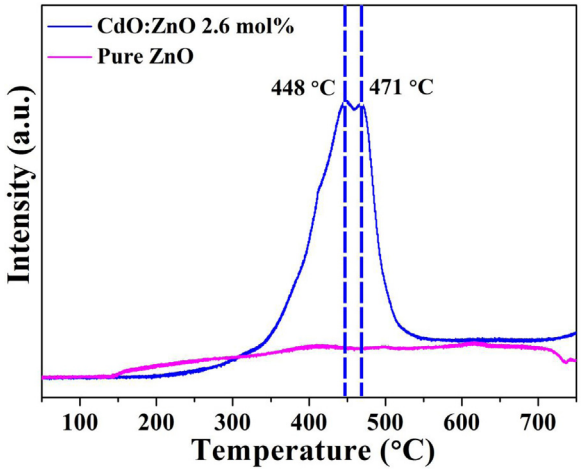

Fig. 10. The H_2-TPR profiles of the samples.

depletion layer and a low resistance are obtained. This will benefit the improvement of sensitivity of heterostructure composites to ethanol.

Secondly, the hollow microspheres architecture can facilitate the gas diffusion and improve the mass transport properties (utility factor), which allows absorbed absorbing gases not only on the surface but also throughout the bulk. Thus leading to an enhanced response and a fast response performance (schematically illustrated in Fig. 9(c and d)) [59,60]. And then, as shown in Fig. 9(e–j), the enhancement in gas sensing properties on CdO/ZnO heterostructure microspheres is also likely to be the result of the synergetic effect of CdO and ZnO [28]. For the monomer CdO/ZnO heterostructure nanoplates, the surfaces of ZnO nanoplates are not completely enclosed by CdO nanoparticles, which results in both of them are highly accessible for the adsorption of oxygen molecules. Considering the depletion layer in CdO/ZnO heterostructure composites, there are two depletion layers in the composites, one depleted layer in the surfaces of ZnO, one depletion layer in the surfaces of CdO nanoparticles. Therefore, when the sensors are exposed to the ethanol gas (Fig. 9(e–g)), the CdO/ZnO heterostructure composites sensor could have a higher response to ethanol (Fig. 9(h–j)) due to more chemisorbed oxygen species will participate in the reaction than that of the pristine ZnO nanoplates and CdO nanoparticles.

Finally, the surface oxidation activity of the pure ZnO and 2.6 mol% CdO:ZnO heterostructure composites are investigated by Temperature Programmed Reduction experiments with H_2 (H_2-TPR), as shown in Fig. 10. TPR spectrum of the 2.6 mol% CdO:ZnO heterostructure composites exhibited two reduction peaks appearing at 448 °C and 471 °C, respectively. However, the pure ZnO do not have obvious reduction peak. This means that more surface active oxygen species could participate in the oxidation–reduction reaction occurring on the surface of the CdO/ZnO composites and thus cause a larger change in sensor resistance. High H_2 consumption peak can be attributed to the better oxidation activity, and resulting in better redox properties [61–64]. The catalytic activity of the CdO/ZnO composites and the mobility of the surface lattice oxygen were all improved by the introduction of CdO. CdO is an n-type semiconductor with a large amount of native defect such as oxygen vacancies, which made oxygen molecules adsorb easily on the surface of the CdO/ZnO heterostructure composites; and the increase in amount of chemisorbed oxygen should be beneficial to the surface reaction activity/kinetics [27,65,66].

5. Conclusion

In this work, the CdO nanoparticles were effectively decorated on the ZnO hollow microspheres by a two-step hydrothermal route. Analysis by XPS and H_2-TPR indicated that the amount of absorb oxygen had been increased by the introduction of CdO. The applications in gas sensors of as-prepared materials were evaluated, the results showed remarkable sensitivity (giving a gas response of 65.6–100 ppm at 250 °C, which was about 16 folder higher than that of pure ZnO) and excellent selectivity toward ethanol. The CdO/ZnO composites possessed a low detection limit (500 ppb). Moreover, the CdO/ZnO composites exhibited good long-term stability for the detection of ethanol. These results suggested that the facile synthesis of CdO/ZnO composites hollow microspheres could offer a new path for developing high performance ethanol sensors.

Acknowledgements

This work is supported by the National Nature Science Foundation of China (No. 61520106003, 61503148, 61327804, 61374218, 61134010), Program for Chang Jiang Scholars and Innovative Research Team in University (No. IRT13018) and National High-Tech Research and Development Program of China (863 Program, No. 2013AA030902 and 2014AA06A505). China Postdoctoral Science Foundation funded project No. 2015M580247. National Key Research and Development Program (NO. 2016YFC0207300).

Appendix A. Supplementary data

Supplementary data associated with this article can be found, in the online version, at http://dx.doi.org/10.1016/j.snb.2017.04.099.

References

[1] Il-D. Kim, A. Rothschild, H.L. Tuller, Advances and new directions in gas-sensing devices, Acta Mater. 61 (2013) 974–1000.
[2] T. Wagner, S. Haffer, C. Weinberger, D. Klaus, M. Tiemann, Mesporous materials as gas sensors, Chem. Soc. Rev. 42 (2013) 4036–4053.
[3] D.R. Miller, S.A. Akbar, P.A. Morris, Nanoscale metal oxide-based heterojunctions for gas sensing: a review, Sens. Actuators B 204 (2014) 250–272.
[4] P.I. Gouma, M. Stanacevic, S. Simon, An overview of the translation of selective semiconducting gas sensors from first results to automotive exhaust gas monitors to a platform for breath-based diagnostics, Transl. Mater. Res. 2 (2015) 4.
[5] S. Das, V. Jayaraman, SnO_2: a comprehensive review on structures and gas sensors, Prog. Mater. Sci. 66 (2014) 112–255.
[6] X.Q. Wang, M.F. Zhang, J.Y. Liu, T. Luo, Y.T. Qian, Shape- and phase-controlled synthesis of In_2O_3 with various morphologies and their gas-sensing properties, Sens. Actuators B 137 (2009) 103–110.
[7] J. Zhang, S.R. Wang, Y. Wang, M.J. Xu, H.J. Xia, S.M. Zhang, W.P. Huang, X.Z. Guo, S.H. Wu, ZnO Hollow spheres: preparation, characterization, and gas sensing properties, Sens. Actuators B 139 (2009) 411–417.
[8] Q.J. Wang, C. Wang, H.B. Sun, P. Sun, Y.Z. Wang, J. Lin, G.Y. Lu, Microwave assisted synthesis of hierarchical Pd/SnO_2 nanostructures for CO gas sensor, Sens. Actuators B 222 (2016) 257–263.
[9] P. Sun, X. Zhou, C. Wang, B. Wang, X.M. Xu, G.Y. Lu, One-step synthesis and gas sensing properties of hierarchical Cd doped SnO_2 nanostructures, Sens. Actuators B 190 (2014) 32–39.
[10] Y. Guan, D.W. Wang, X. Zhou, P. Sun, H. Wang, J. Ma, G.Y. Lu, Hydrothermal preparation and gas sensing properties of Zn doped SnO_2 hierarchical architectures, Sens. Actuators B 191 (2014) 45–52.
[11] A.A. Firooz, T. Hyodo, A.R. Mahjoub, A.A. Khodadadi, Y. Shimizu, Synthesis and gas-sensing properties of nano and mesoporous MoO_3-doped SnO_2, Sens. Actuators B 147 (2010) 554–560.
[12] X.Y. Xue, L.L. Xing, Y.J. Chen, S.L. Shi, Y.G. Wang, T.H. Wang, Synthesis and H_2S sensing properties of CuO-SnO_2 core/shell pn-junction nanorods, J. Phys. Chem. C 112 (2008) 12157–12160.
[13] D.W. Chu, Y.P. Zeng, D.L. Jiang, Y. Masuda, In_2O_3-SnO_2 nano-toasts and nanorods: precipitation preparation, formation mechanism, and gas sensitive properties, Sens. Actuators B 137 (2009) 630–636.
[14] X.C. Ma, H.Y. Song, C.S. Guan, Enhanced ethanol sensing properties of ZnO-doped porous SnO_2 hollow nanospheres, Sens. Actuators B 188 (2013) 193–199.

[15] C.L. Zhu, Y.J. Chen, R.X. Wang, L.J. Wang, M.S. Cao, X.L. Shi, Synthesis and enhanced ethanol sensing properties of α-Fe_2O_3/ZnO heteronanostructures, Sens. Actuators B 140 (2009) 185–189.
[16] H.L. Tian, H.Q. Fan, G.Z. Dong, L.T. Ma, J.W. Ma, NiO/ZnO p–n heterostructures and their gas sensing properties for reduced operating temperature, RSC Adv. 6 (2016) 109091–109098.
[17] T.S. Wang, Z.S. Huang, Z.D. Yu, B.Q. Wang, H. Wang, P. Sun, H. Suo, Y. Gao, Y.F. Sun, T. Li, G.Y. Lu, Low operating temperature toluene sensor based on novel α-Fe_2O_3/SnO_2 heterostructure nanowires arrays, RSC Adv. 6 (2016) 52604–52610.
[18] T. Chen, Z.L. Zhou, Y.D. Wang, Effects of calcining temperature on the phase structure and the formaldehyde gas sensing properties of CdO-mixed In_2O_3, Sens. Actuators B 135 (2008) 219–223.
[19] J.H. Kim, W.S. Kim, K.J. Yong, CuO/ZnO heterostructured nanorods: photochemical synthesis and the mechanism of H_2S gas sensing, J. Phys. Chem. C 116 (2012) 15682–15691.
[20] Y.D. Zhu, Y.Y. Wang, G.T. Duan, W.H. Zhang, Y. Li, G.Q. Liu, L. Xu, W.P. Cai, In situ growth of porous ZnO nanosheet-built network film as high-performance gas sensor, Sens. Actuators B 221 (2015) 350–356.
[21] X.Z. Wang, W. Liu, J.R. Liu, F.L. Wang, J. Kong, S. Qin, C.Z. He, L.Q. Luan, Synthesis of nestlike ZnO hierarchically porous structures and analysis of their gas sensing properties, ACS Appl. Mater. Interface 4 (2012) 817–825.
[22] D.W. Wang, S.S. Du, X. Zhou, B. Wang, J. Ma, P. Sun, Y.F. Sun, G.Y. Lu, Template-free synthesis and gas sensing properties of hierarchical hollow ZnO microspheres, CrystEngComm 15 (2013) 7438–7442.
[23] Y. Ding, Y. Wang, L.C. Zhang, H. Zhang, Y. Lei, Preparation characterization and application of novel conductive NiO-CdO nanofibers with dislocation feature, J. Mater. Chem. 22 (2012) 980–986.
[24] D.S. Raja, T. Krishnakumar, R. Jayaprakash, T. Prakash, G. Leonardi, G. Neri, CO sensing characteristics of hexagonal-shaped CdO nanostructures prepared by microwave irradiation, Sens. Actuators B 171–172 (2012) 853–859.
[25] D.M. Carballeda-Galicia, R. Castanedo-Pïerez, O. Jimíenez-SandovalU, S. Jimíenez-Sandoval, G. Torres-Delgado, C.I. Zíu˜niga-Romero, High transmittance CdO thin films obtained by the sol-gel method, Thin Solid Films 371 (2000) 105–108.
[26] M. Ocampo, A.M. Fernandez, P.J. Sebastian, Transparent conducting CdO films formed by chemical bath deposition, Sci. Technol. 8 (1993) 750–751.
[27] W.S. Kim, M.K. Beak, K.J. Yong, Fabrication of ZnO/CdS, ZnO/CdO core/shell nanorod arrays and investigation of their ethanol gas sensing properties, Sens. Actuators B 223 (2016) 599–605.
[28] S.G. Ban, X.H. Liu, T. Ling, C.K. Dong, J. Yang, X.W. Du, CdO nanoflake arrays on ZnO nanorod arrays for efficient detection of diethyl ether, RSC Adv. 6 (2016) 2500.
[29] H.-J. Kim, H.-M. Jeong, T.-H. Kim, J.-H. Chung, Y.C. Kang, J.-H. Lee, Enhanced ethanol sensing characteristics of In_2O_3-decorated NiO hollow nanostructures via modulation of hole accumulation layers, ACS Appl. Mater. Interfaces 6 (2014) 18197–18204.
[30] K.-Il. Choia, H.-J. Kim, Y.C. Kang, J.-H. Lee, Ultraselective and ultrasensitive detection of H_2S in highly humid atmosphere using CuO-loaded SnO_2 hollow spheres for real-time diagnosis of halitosis, Sens. Actuators B 194 (2014) 371–376.
[31] Y.L. Wang, X.B. Cui, Q.Y. Yang, J. Liu, Y. Gao, P. Sun, G.Y. Lu, Preparation of Ag-loaded mesoporous WO_3 and its enhanced NO_2 sensing performance, Sens. Actuators B 225 (2016) 544–552.
[32] X. Zhou, Y. Xiao, M. Wang, P. Sun, F.M. Liu, X.S. Liang, X.W. Li, G.Y. Lu, Highly enhanced sensing properties for ZnO nanoparticle-decorated round-edged α-Fe_2O_3 hexahedrons, ACS Appl. Mater. Interface 7 (2015) 8743–8749.
[33] C.J.F. Moulder, Handbook of X-ray photoelectron spectroscopy: a reference book of standard spectra for identification and interpretation of XPS data, perkin-elmer corporation, physical electronics division, USA (1992).
[34] J.C. Dupin, D. Gonbeau, P. Vinatier, A. Levasseur, Systematic XPS studies of metal oxides hydroxides, and peroxides, Phys. Chem. Chem. Phys. 2 (2000) 1319–1324.
[35] J.C. Belmonte, J. Manzano, J. Arbiol, A. Cirera, J. Puigcorbe, A. Vila, N. Sabate, I. Gracia, C. Cane, J.R. Morante, Micromachined twin gas sensor for CO and O_2 quantification based on catalytically modified nano-SnO_2, Sens. Actuators B 114 (2006) 881–892.
[36] L. Bie, X.N. Yan, J. Yin, Y.Q. Duan, Z.H. Yuan, Nanopillar ZnO gas sensor for hydrogen and ethanol, Sens. Actuators B 126 (2007) 604–608.
[37] D.X. Ju, H.Y. Xu, J. Zhang, J. Guo, B.Q. Cao, Direct hydrothermal growth of ZnO nanosheets on electrode for ethanol sensing, Sens. Actuators B 201 (2014) 444–451.
[38] L.J. Zhou, C.G. Li, X.X. Zou, J. Zhao, P.P. Jin, L.L. Feng, M.H. Fan, G.D. Li, Porous nanoplate-assembled CdO/ZnO composite microstructures: a highly sensitive material for ethanol detection, Sens. Actuators B 197 (2014) 370–375.
[39] X.Y. Cai, D. Hu, S.J. Deng, B.Q. Han, Y. Wang, J.M. Wu, Y.D. Wang, Isopropanol sensing properties of coral-like ZnO-CdO composites by flash preparation via self-sustained decomposition of metal–organic complexes, Sens. Actuators B 198 (2014) 402–410.
[40] J.G. Guo, Z. Li, H.X. Xi, Y.S. He, B.G. Wang, Activity comparison of three transition metal catalysts used in the catalytic combustion of VOCs, J. South China Univ. Technol. (Nat. Sci. Ed.) 32 (2004) 5.
[41] W. Zen, T.M. Liu, Gas-sensing properties of SnO_2-TiO_2-based sensor for volatile organic compound gas and its sensing mechanism, Phys. B 405 (2010) 1345–1348.
[42] A.P. Lee, B.J. Reedy, Temperature modulation in semiconductor gas sensing, Sens. Actuators B 60 (1999) 35–42.
[43] J. Mizsei, How can sensitive and selective semiconductor gas sensors be made, Sens. Actuators B 23 (1995) 173–176.
[44] B.A. Tichenor, M.A. Palazzolo, Destruction of volatile organic compounds via catalytic incineration, Environ. Prog. 6 (1987) 172–176.
[45] A.S. Kamble, R.C. Pawar, N.L. Tarwal, L.D. More, P.S. Patil, Ethanol sensing properties of chemosynthesized CdO nanowires and nanowalls, Mater. Lett. 65 (2011) 1488–1491.
[46] A.S. Kamblea, R.C. Pawara, J.Y. Patil b, S.S. Suryavanshib, P.S. Patil, From nanowires to cubes of CdO: ethanol gas response, J. Alloys Compd. 509 (2011) 1035–1039.
[47] K. Sankarasubramanian, M. Sampath, J. Archana, K. Sethuraman, K. Ramamurthi, Y. Hayakawa, Influence of substrate temperature on ethanol sensing properties of CdO thin films prepared by facile spray pyrolysis method, J. Mater. Sci: Mater. Electron. 26 (2015) 955–961.
[48] X.W. Li, W. Feng, Y. Xiao, P. Sun, X.L. Hu, K. Shimanoe, G.Y. Lu, N. Yamazoe, Hollow zinc oxide microspheres functionalized by Au nanoparticles for gas sensors, RSC Adv. 4 (2014) 28005–28010.
[49] A. Hastir, N. Kohli, R.C. Singh, Temperature dependent selective and sensitive terbium doped ZnO nanostructures, Sens. Actuators B 231 (2016) 110–119.
[50] N.L. Tarwal, A.R. Patil, N.S. Harale, A.V. Rajgure, S.S. Suryavanshi, W.R. Bae, P.S. Patil, J.H. Kim, J.H. Jang, Gas sensing performance of the spray deposited Cd-ZnO thin films, J. Alloys Compd. 598 (2014) 282–288.
[51] S.H. Yan, S.Y. Ma, W.Q. Li, X.L. Xu, L. Cheng, H.S. Song, X.Y. Liang, Synthesis of SnO_2-ZnO heterostructured nanofibers for enhanced ethanol gas-sensing performance, Sens. Actuators B 221 (2015) 88–95.
[52] L.M. Huang, H.Q. Fan, Room-temperature solid state synthesis of ZnO/α-Fe_2O_3 hierarchical nanostructures and their enhanced gas-sensing properties, Sens. Actuators B 171–172 (2012) 1257–1263.
[53] C.W. Na, S.-Y. Park, J.-H. Chung, J.-H. Lee, Transformation of ZnO nanobelts into single-crystalline Mn_3O_4 nanowires, ACS Appl. Mater. Interfaces 4 (2012) 6565–6572.
[54] D. Sivalingam, J.B. Gopalakrishnan, J.B.B. Rayappan, Nanostructured mixed ZnO and CdO thin film for selective ethanol sensing, Mater. Lett. 77 (2012) 117–120.
[55] Z.F. Dai, C.S. Lee, B.Y. Kim, C.H. Kwak, J.W. Yoon, H.M. Jeong, J.H. Lee, Honeycomb-like periodic porous $LaFeO_3$ thin film chemiresistors with enhanced gas-sensing performances, Sens. Actuators B 3 (2014) 13217.
[56] J. Yu, S.J. Ippolito, W. Wlodarski, M. Strano, K. Kalantar-zadeh, Nanorod based schottky contact gas sensors in reversed bias condition, Nanotechnology 2126 (2010) 265502.
[57] T.T. Yu, X.F. Zhang, Y.M. Xu, X.L. Cheng, S. Gao, H. Zhao, L.H. Huo, Low concentration H_2S detection of CdO-decorated hierarchically mesoporous NiO nanofilm with wrinkle structure, Sens. Actuators B 230 (2016) 706–713.
[58] J.X. Zhang, G.X. Zhu, X.P. Shen, Z.Y. Ji, K.M. Chen, α-Fe_2O_3 nanospindles loaded with ZnO nanocrystals: synthesis and improved gas sensing performance, Cryst. Res. Technol. 7 (2014) 452–459.
[59] N. Yamazoe, K. Suemastu, K. Shimanoe, Surface chemistry of neat tin oxide sensor for response to hydrogen gas in air, Sens. Actuators B 227 (2016) 403–410.
[60] M.M. Arafat, B. Dinan, Sheikh A. Akbar, A.S.M.A. Haseeb, Gas sensors based on one dimensional nanostructured metal-oxides: a review, Sensors 12 (2012) 7207–7258.
[61] J.Y.Z. Chiou, C.L. Lai, S.W. Yu, H.-H. Huang, C.-L. Chuang, C.B. Wan, Effect of Co, Fe and Rh addition on coke deposition over Ni/$Ce_{0.5}Zr_{0.5}O_2$ catalysts for steam reforming of ethanol, Int. J. Hydrogen Energy 39 (2014) 20689–20699.
[62] T.K. Xu, J. Zou, W.T. Tao, S.Y. Zhang, L. Cui, F.L. Zeng, D.Z. Wang, W.J. Cai, Co-nanocasting synthesis of Cu based composite oxide and its promoted catalytic activity for methanol steam reforming, Fuel 183 (2016) 238–244.
[63] H. Bake, S.F. Zaman, Y.A. Alhamed, A.A. Al-Zahrani, M.A. Daous, S.U. Rather, H. Drissb, L.A. Petrovb, Partial oxidation of methanol over Au/CeO_2–ZrO_2 and Au/CeO_2–ZrO_2–TiO_2 catalysts, RSC Adv. 6 (2016) 22555.
[64] C. Pojanavaraphan, A. Luengnaruemitchai, E. Gulari, Effect of catalyst preparation on Au/$Ce_{1-x}Zr_xO_2$ and Au–Cu/$Ce_{1-x}Zr_xO_2$ for steam reforming of methanol, Int. J. Hydrogen Energy 38 (2013) 1348–1362.
[65] N. Han, X.F. Wu, D.W. Zhang, G.L. Shen, H.D. Liu, Y.F. Chen, CdO activated Sn-doped ZnO for highly sensitive, selective and stable formaldehyde sensor, Sens. Actuators B 152 (2011) 324–329.
[66] J. Su, X.X. Zou, Y.C. Zou, G.D. Li, P.P. Wang, J.S. Chen, Porous titania with heavily self-doped Ti^{3+} for specific sensing of CO at room temperature, Inorg. Chem. 52 (2013) 5924–5930.

Biographies

Tianshuang Wang received his BS degree from the Electronics Science and Engineering department, Jilin University, China in 2015. Presently, he is a graduate student and interested in the synthesis and characterization of the semiconducting functional materials and gas sensors.

Xueying Kou received her BS degree from the Science department, Changchun University of Science and Technology, China in 2015. Presently, she is a graduate student and interested in the synthesis and characterization of the semiconducting functional materials and gas sensors.

Liupeng Zhao He is currently working toward the MS degree in the Electronics Science and Engineering department, Jilin University. His research interests include the synthesis of functional materials and their applications in gas sensors.

Chang Liu received the MS degree in Department of Electronic Sciences and Technology in 2015. Now she is currently working toward the Ph.D degree in the Electronics Science and Engineering department, Jilin University. Her research interests include the synthesis of functional materials and their applications in gas sensors.

Peng Sun received his PhD degree from the Electronics Science and Engineering department, Jilin University, China in 2014. Now, he is engaged in the synthesis and characterization of the semiconducting functional materials and gas sensors.

Yue Wang received his PhD degree from Jilin University, China in 1991. He then joined the State Key Lab of Supramolecular Structure and Materials in Jilin University as an assistant professor. He is currently a full professor in the State Key Lab of Supramolecular Structure and Materials in Jilin University. His research interests are organic electroluminescence, thin film transistor and solar cell materials and devices.

Kengo Shimanoe has been a professor at Kyushu University since 2005. He received a B. Eng. degree in applied chemistry in 1983 and a M. Eng. degree in 1985 from Kagoshima University and Kyushu University, respectively. He joined Nippon Steel Corp. in1985, and received a Dr. Eng. degree in1993 from Kyushu University. His current research interests include the development of gas sensors and other functional devices.

Noboru Yamazoe had been a professor at Kyushu University since 1981 until he retired in 2004. He received his M. Eng. degree in applied chemistry in 1963 and his Dr. Eng. Degree in1969 from Kyushu University. His research interests were directed mostly to the development and application of functional inorganic materials.

Geyu Lu received his BS and MS degree in electronic sciences from Jilin University, China in 1985 and 1988, respectively, and PhD degree in 1998 from Kyushu University in Japan. Now he is a professor of Jilin University, China. Presently, he is interested in the development of functional materials and chemical sensors.